STUDIES OF COAL REACTIVITY FOR DIRECT LIQUEFACTION*

H. P. Stephens and R. J. Kottenstette

Sandia National Laboratories
Process Research Division
Albuquerque, New Mexico USA

SAND--90-0141C

DE91 002699

INTRODUCTION

Direct liquefaction of coal involves the conversion of a hydrogen-poor organic solid to a liquid richer in hydrogen by a complex set of bond scission and hydrogen transfer reactions. Although the reactivity of coal is obviously determined substantially by its chemical structure, it has been difficult to correlate the reactivity of coal for direct liquefaction processes with coal structure because of its complex and heterogeneous nature. Recent models of coal structure (1-3) depict the organic portion as a three-dimensionally cross-linked macromolecular network containing dissolved, extractable molecules of relatively low molecular weight. The macromolecular network can be described as groups of heteroatom-containing polycyclic, aromatic and hydroaromatic ring structures joined by hydrogen bonds and covalent linkages consisting of short chains of carbon, oxygen, sulfur or nitrogen atoms (4-7). The portion of these various components, the sizes of the ring structures and covalent linkages, and the number of groups between hydrogen bonds and aliphatic crosslinks, varies with coal origin and rank.

This paper presents a preliminary report on a continuing effort to quantify the reactivity of coal for direct liquefaction reactions in terms of the utilization of hydrogen, the selectivity to products and the properties of the products formed. Liquefaction processes are aimed at maximizing the yield of distillate that can serve as hydrocarbon fuels and chemical feedstocks. Direct coal liquefaction processes involve heating a slurry of coal in a process-derived solvent to temperatures typically not exceeding about 450°C in the presence of high pressure hydrogen. The solvent is a hydrogenated portion (usually a heavy distillate cut) of the product which acts both as

---

MASTER

a process vehicle and a hydrogen transfer agent. All modern processes use at least two reactors (thermal or catalytic) in series to optimize several functions of the process: conversion of coal to soluble products consisting primarily of high molecular weight non-distillate material; conversion of the soluble primary products to distillates of lower molecular weight; hydrogenation of the products and removal of heteroatoms; and production of the recycle solvent.

One of the most important aspects of coal liquefaction is control of the dissolution step, which involves the transition from solid coal to initial dissolved products, as coal is reacted with the process donor solvent and hydrogen at elevated temperatures and pressures, and in some cases in the presence of a catalyst. Although significant dissolution of coal occurs in first-stage reactor preheaters, often at temperatures as low as 300°C (8), onset and rate of dissolution depends on coal rank, process solvent composition and other parameters. Relative to subsequent steps, dissolution is a fast process that involves both physical and chemical changes in the coal. Penetration and swelling by the process solvent occurs, resulting in extraction of organics dissolved in the macromolecular network and changes in the morphology of coal particles. At the same time, thermal rupture of weak bonds to form free radicals (9-11) results in the formation of the initial high molecular weight depolymerized products, referred to as "preasphaltenes". Subsequently, a series of reactions, including radical induced cleavage (12,13) of stronger bonds, occurs to yield products, asphaltenes and oils, of lower molecular weight. In parallel with these reactions, gas primarily consisting of CO, CO_2, H_2S, H_2O, and C_1-C_4 hydrocarbons is generated. The reactive free radicals formed in the dissolution step of coal liquefaction may be stabilized by reaction either with hydrogen, primarily from a hydroaromatic donor molecule or with another aryl free radical. While reaction with hydrogen leads to the desired low molecular weight products, reaction with an aryl free radical produces undesirable refractory high molecular weight material responsible for reduced yields of liquids, catalyst deactivation (14) and problems with process operability, for example preheater plugging (15).

Thus conversion of high molecular weight coal molecules into lower molecular weight moieties by bond breaking reactions, concurrent with efficient hydrogen transfer, is essential for the production of high yields of distillate products. The reactivity of coal for liquefaction processes will depend, in general, on the processing conditions, the strength of the bonds linking the lower molecular weight coal moieties together, and

the amount of donor hydrogen available. This study seeks to better describe: 1) how hydrogen consumed during liquefaction is distributed among product groups; 2) coal reactivity in terms of a relationship defining the selectivity to products formed during liquefaction; and 3) the relation of coal structure to reactivity for liquefaction reactions. Because of the limited space for reporting this effort in this special edition of Fuel, the experimental methods, calculations and data are presented in abbreviated form in order to focus on interpretation and discussion of the results in terms of coal structure and reactivity.

EXPERIMENTAL

Two sets of coal liquefaction experiments, outlined here and described in more detail in the following sections, were performed. The first set consisted of four pairs of batch reactions (16 g of coal/solvent slurry per pair, 1:2 coal:solvent ratio), carried out under mild (390°C, 10 min) and moderate (418°C, 30 min), catalyzed and uncatalyzed liquefaction conditions. These experiments were designed to determine the molecular weight and elemental composition of product groups, and to prepare samples for calibration of the high pressure liquid chromatography (HPLC) apparatus used to analyze the product distributions for the second set of experiments. Reaction products from these experiments were separated into three groups according to molecular size, and were subjected to elemental analysis and to vapor phase osmometry to determine the number-average molecular weights. The second set of 18 experiments, performed over a wider range of reaction conditions, was designed to investigate the selectivity to product groups and the impact of hydrogen availability on liquefaction product distributions. These experiments were performed under catalyzed and uncatalyzed conditions with different solvents, different solvent-to-coal ratios, and over a wide range of temperatures (368-426°C) and reaction times (5-74 min).

Materials
Except as noted below, liquefaction reactions were performed with Illinois No. 6 coal (Burning Star) and a liquefaction process-derived heavy distillate solvent (H/C = 1.05), with a solvent-to-coal ratio of 2:1. To study the impact of a high-hydrogen content, coal-derived solvent on gas-phase hydrogen consumption and product distributions, several experiments were performed with a hydrogenated creosote oil (H/C = 1.16). To test the effects of solvent-to-coal ratio, several other experiments were performed

with heavy distillate solvent-to-coal ratios of 4:1 and 8:1. Catalyzed experiments were performed with addition of a commercial Co-Mo/alumina catalyst, ground to -200 mesh to eliminate the effects of intraparticle diffusion. High purity hydrogen was use in all experiments.

Apparatus and Procedure

All liquefaction reactions were performed in batch microautoclaves equipped with thermocouples and pressure transducers, and having slurry capacities. of approximately 8 g and gas volumes of 35 cm³. These are described in detail elsewhere (16). Four reactors could be operated simultaneously. After the reactors were charged with slurry, they were pressurized to 5.52 MPa with hydrogen. The reactors were then mounted on an agitation apparatus and heated to temperature in a fluidized sandbath while being agitated with a wrist action motion at 200 cycles/min during the reaction period. Temperatures of the slurries and pressures of the gas phase were accurately monitored and recorded by a digital data acquisition system during the course of the experiments. Following the heating period, the reaction vessels were quenched in water to ambient temperature, the resulting temperatures and pressures were recorded, a gas sample was taken, and the condensed-phase reaction product was removed for analysis.

Product Analyses

Gas samples of all reactions were analyzed for mole percentages of CO, CO_2, H_2S, and C_1 - C_4 hydrocarbons with a gas chromatograph, which was calibrated with standard mixtures of hydrocarbon gases and H_2S in hydrogen. Hydrogen in the samples was determined as the remainder of the product gas mixture. The quantity of each gas produced was calculated, using an ideal gas law calculation, from the mole percent in the gas sample and the post-reaction vessel temperature and pressure. Hydrogen consumed during the reaction was obtained as the difference between the initial charge and hydrogen remaining after the reactor was quenched.

Products from the first set of four pairs of experiments were quantitatively separated by Soxhlet extraction into four solubility classes: tetrahydrofuran (THF) insoluble organic material (IOM), THF, toluene and pentane solubles. The THF solubles (often referred to as "preasphaltenes") and toluene solubles ("asphaltenes") were then further separated into three fractions: high, intermediate, and low molecular weight (mw)

(mw) groups by HPLC using a preparative-scale size exclusion column. An ultraviolet (uv) absorbance detector was used to monitor the progress of the separation, and product cuts were made at retention times previously identified by prominent inflections in the absorbance spectrum. Each of these product groups and the pentane soluble product for the four pairs of experiments were then analyzed for carbon, hydrogen, nitrogen and sulfur content (oxygen taken as the difference), and also subjected to vapor phase osmometry (where sufficient sample was available) to determine the number-average molecular weight. The high mw fraction of the preasphaltenes, the intermediate mw fraction of the asphaltenes, and the pentane soluble "oil" of each pair of experiments were used, as described below, to calibrate the HPLC apparatus for analysis of the product slurry of subsequent experiments.

Reaction product slurries of the second set of experiments were analyzed for IOM, high mw, intermediate mw, and low mw products by THF solubility and HPLC analysis. A 0.2 g subsample was mixed with 50 ml of THF, filtered to obtain the weight of insols, and brought to 100 ml with additional THF. Chromatograms of the filtrate were obtained with a high pressure solvent delivery system, a 10 nm microstyragel gel permeation column, and a uv absorbance detector. Chromatographic data was collected and analyzed with a digital acquisition/desktop computer system. The uv absorbance response factors at 254 nm for the product groups were determined using THF solutions prepared by dissolving weighed portions of the calibration samples described above. The response factors were proportional to the area under the chromatographic curve divided by the calibration sample weight. Because the values of the response factors were somewhat dependent on reaction conditions, calibration samples were chosen which represented reaction conditions best matched to those of the sample. Sample chromatogram area measurements and response factors were used to calculate the percentages of high, intermediate, and low mw products. Conversions and product distributions were calculated on a dry, mineral matter free (dmmf) basis.

RESULTS AND DISCUSSION

Hydrogen Consumption

Analysis of the data from the first set of four pairs of experiments allowed quantification of the disposition of gas-phase hydrogen consumed during the reactions. Table 1
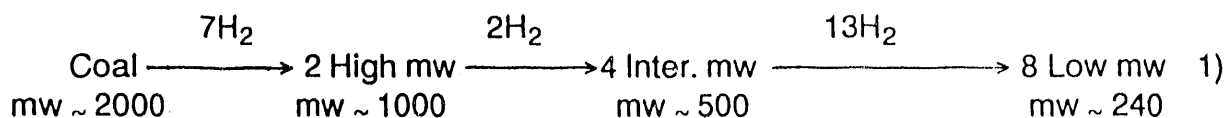
presents these results in terms of the hydrogen content of the reaction products (IOM, high, intermediate, and low mw condensed-phase products and hydrocarbon gases), and the amount consumed by solvent hydrogenation and heteroatom elimination. These data are given in the lines labeled "H Accounting." Also shown are the reaction conditions; product yields (dmmf coal basis conversions); the H/C atomic ratios for the condensed-phase products and coal; and hydrogen uptake calculated from product hydrogen content, heteroatom elimination and solvent hydrogenation, and hydrogen uptake determined from gas-phase consumption.

Hydrogen consumed from the gas phase was calculated as described in the Experimental Section. Product hydrogen contents and hydrogen consumption due to solvent hydrogenation and heteroatom elimination were determined in the following manner. The hydrogen contents of the products were calculated from the elemental analyses of the product groups and the post-reaction gas phase composition. Hydrogen consumed by the solvent was calculated from the yield of low mw product, the weight of the starting solvent, and the difference in the hydrogen content of the post-reaction pentane solubles (which includes both low mw product and hydrogenated solvent) and that for the unreacted heavy distillate solvent. With respect to heteroatom elimination, the elemental analyses of the condensed-phase products showed that there was little nitrogen elimination, and that the oxygen contents of the high and intermediate molecular weight products for all four pairs of experiments were nearly the same as the coal. However, depending on the reaction conditions, the low molecular weight products were found to contain 1/2 to 3/4 of the oxygen content of the coal. The hydrogen associated with oxygen removal was estimated from the total amount of oxygen eliminated and the CO and CO_2 formed in the gas-phase products. Hydrogen associated with sulfur removal was calculated from the analyzed content of H_2S in the gas phase. Note that hydrogen consumptions calculated from product hydrogen contents, heteroatom elimination and solvent hydrogenation agree, within the limits of experimental error, with those determined from gas-phase consumption. This corroborates the methods used to assign hydrogen consumption to solvent hydrogenation and heteroatom elimination.

From an examination of Table 1, a number of observations regarding hydrogen consumption in these direct coal liquefaction experiments can be made: 1) For the same reaction conditions, the catalyzed reactions consumed three times as much gas-phase hydrogen as the uncatalyzed reactions. 2) For the catalyzed experiments,

hydrogen consumed from the gas phase was primarily accounted for by an increase in the solvent hydrogen content and uptake by the coal to form products richer in hydrogen. Heteroatom removal consumed only a small amount of hydrogen. 3) The uncatalyzed reactions, for which there was much less gas-phase hydrogen consumption, showed several indications of hydrogen starvation, including poor conversions to low mw product, solvent adduction (17) for the experiment performed at 390°C, and lower H/C ratios for the entire condensed-phase product slate.

Although the reactions involved in the liquefaction of coal are complex, a description of the process in terms of a simple series of reaction steps to form non-gaseous products is useful in order to obtain a qualitative representation of the stoichiometry of hydrogen uptake. The following stoichiometry for hydrogen consumption was calculated from the measured molecular weights of soluble condensed-phase products (M_n = 1070±470 for high mw; M_n = 506±9 for intermediate mw; and M_n = 237±47 for low mw) and the elemental analyses of the product groups resulting from reactions performed under conditions of adequate hydrogen availability, that is, the catalyzed reactions. The value 2000 for the molecular weight (between covalent crosslinks) of coal was chosen on the basis of recent molecular (6,7) and cross-linked macromolecular network (18) models of coal structure.

$$\begin{array}{cccc} & 7H_2 & 2H_2 & 13H_2 \\ \text{Coal} \xrightarrow{\hspace{1cm}} & 2\text{ High mw} \xrightarrow{\hspace{1cm}} & 4\text{ Inter. mw} \xrightarrow{\hspace{1cm}} & 8\text{ Low mw} \quad 1) \\ \text{mw} \sim 2000 & \text{mw} \sim 1000 & \text{mw} \sim 500 & \text{mw} \sim 240 \end{array}$$

The above stoichiometry indicates that a relatively high rate of hydrogen consumption occurs early in the reaction sequence, as coal forms high mw THF soluble species. This is consistent with observed rates of gas-phase hydrogen uptake as a function of reaction time and reports of other investigators (19). Although the reason for this is not known, recent results of modeling of coal structure using computer-aided molecular design (CAMD) coupled with molecular dynamics calculations to obtain the van der Waals energy for intramolecular attractions (20,21), and studies of bituminous coal anisotropy and aromatic-aromatic interactions (22) offer one possible explanation. Both of these studies indicate that non-covalent, dipole-based interactions between the aromatic groups in coal contribute substantially to the energy involved in tightly packing aromatic clusters of the coal molecular structure. A significant portion of the relatively high hydrogen consumption during the early stages of the coal liquefaction process may, by the hydrogenation of aromatic structures, serve to reduce the

intramolecular forces between rings, thus relaxing the molecular structure. This would allow better penetration of hydroaromatic solvent species into the high molecular weight moieties to induce bond scission reactions and transfer hydrogen to free radicals formed by homolytic scission of weak bonds such as benzylic ether linkages. In light of this explanation, it is interesting to note that the conversion of the solublized high mw species to intermediate mw species requires only enough hydrogen to break one bond per high mw specie. Additional hydrogen may not be required because the molecular structure of the high mw species is relaxed enough to provide adequate solvent penetration for cleavage of strong bonds by radical induced scission (12,13). The higher hydrogen consumption for the formation of low mw products results from a combination of covalent bond scission, hydrogenation of aromatic rings, and heteroatom elimination.
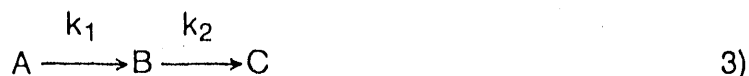
Selectivity to Products

Product selectivity relationships for direct coal liquefaction have been difficult to describe precisely, not only because of the complexity of the reaction mixtures, but also because of the difficulty of comparing the results of experiments performed under different reaction conditions. The approach to selectivity relationships described here is based on a ternary product distribution diagram which relates product and by-product conversions grouped according to molecular weight. Ternary product distribution diagrams with reaction paths represented by empirical hyperbolic relationships of the form

$$y = x(1-x)/(a+bx) \qquad\qquad 2)$$

have been used to describe selectivity relationships for complex reactions (23-25). The variables y and x represent the by-product (intermediate mw product) and product (low mw product) conversions respectively, and a and b are empirical constants. Except for two studies reported by Stephens (26,27), the application of ternary diagrams to direct coal liquefaction has been unexplored. Although empirical relations such as equation 2 may be used to fit conversion data, representation in terms of a specific chemical reaction path and interpretation in terms of kinetic equations may allow better correlation with models of coal structure. Use of a simple reaction pathway, that of consecutive first-order reactions, is explored here for representing product distributions for the conversion of coal.

For a first order series reaction path of the form

$$A \xrightarrow{k_1} B \xrightarrow{k_2} C \qquad\qquad 3)$$

where A is the reactant and B and C represent the by-products and products, the selectivity S can be defined as the ratio of the rate constants, $S=k_1/k_2$. Upon solving the kinetic equations, the following equations may be derived to relate the percent conversion of A to B ($y = 100\,B/A_o$) and A to C ($x = 100\,C/A_o$), where A_o represents the initial amount of A:

$$y = S(x-100) \pm S(100-x-y)^{1/S}; \ S \neq 1 \qquad\qquad 4)$$

$$y = (y+x-100) \ln(y+x-100); \ S = 1 \qquad\qquad 5)$$

Figure 1 is an example of a ternary diagram for the series reaction represented by equation 3, showing conversion relationships for several values of S. Although reaction time is eliminated from these curves, increasing the reaction time moves the composition of a reaction mixture along a product distribution curve from left to right. The effect of temperature upon the selectivity S can be determined from the Arrhenius expression for first-order reactions:

$$k = F\,e^{-E/RT} \qquad\qquad 6)$$

where F is the frequency factor and E is the Activation energy. The temperature dependence of S is given by:

$$S = k_1/k_2 = (F_1/F_2)\,e^{(E_2-E_1)/RT} \qquad\qquad 7)$$

Thus S is constant over a range of temperatures only if E_2 is equal to E_1 over that range. In this case, increasing reaction temperature also moves the composition along a selectivity or processing curve, from left to right. For reactions for which E_2 and E_1 are not equal, the selectivity changes with temperature. In this case, data for experiments performed over a range of temperatures cannot be fit by a single product distribution curve.

If y represents the percent conversion of coal to intermediate mw products and x the percent conversion to low mw products, the course of direct coal liquefaction processes can be represented on a ternary diagram. The composition of the product mixture is given by the fractions explicitly represented by the x and y axes and a remaining fraction (high mw product, IOM or unreacted coal) is given by the difference 100-(x+y). Thus for direct liquefaction the consecutive reactions may be represented as:

$$[\text{Coal+IOM+High mw}] \xrightarrow{k_1} \text{Intermediate mw} \xrightarrow{k_2} \text{Low mw} \qquad 8)$$

The data for the second set of experiments can now be interpreted in terms of the analysis given above. The reaction conditions, condensed-phase product distributions, and gas-phase hydrogen consumptions for the second set of 18 experiments are given in Table 2. It was previously reported (27) that data plotted on a ternary diagram in terms of conversion of coal to intermediate mw and low mw product groups could be represented by a single curve of approximately hyperbolic functionality. The curve could be used to represent the product compositions over a wide range of experimental conditions, as long as there was an adequate supply of hydrogen available from catalyzc ⅃ transfer from the gas phase, a solvent rich in donor hydrogen, or a high solvent-to-coal ratio. However, no attempt was made to fit the data to equations 4 and 5, derived from kinetic expressions. Conversion data for experiments in which there was an adequate supply of hydrogen (experiments 6-18) are shown plotted on the ternary diagram given in Figure 2, along with the curve representing the least squares fit to equation 4. Data from experiments 1-5 were not used for this plot because of indications of hydrogen starvation, including solvent adduction and poor yields of low mw product. As can be seen from Figure 2, only an approximate fit to equation 4 could be achieved. Examination of Figure 2 indicates that the poor fit results from yields of the low mw product which appear to be too large, thus skewing the data to the right relative to the hyperbolic curve of the ternary diagram. However, if the values for conversion to low mw product are reduced by 9%, an excellent fit is achieved, with S=1.3, as shown in Figure 3.

Rationalization for this reduction in the low mw product is supported by the recent characterization of the nature and amount of low molecular weight material entrapped within the coal macromolecular network. Although there is considerable controversy

and debate on this subject (28), it has been reported (29) that 8.2 wt % of Illinois No. 6 coal may be extracted with an azeotropic mixture of benzene and methanol. Other investigators (30) estimate extractable material to be 5 to 15% for bituminous coals. Therefore it is reasonable to assume that about 9% of the low mw product was rapidly released from the coal matrix by extraction with the liquefaction solvent, rather than by the sequence of rate-limiting kinetic steps of equation 8.

Coal Structure and Reactivity

In summary, observations resulting from this study of the reactivity of coal for conversion to liquid products by a direct liquefaction process can be rationalized by various aspects of a macromolecular network model for coal structure:

(1) The stoichiometry of hydrogen consumption (equation 1) as a function of product distributions, grouped by molecular weight, indicates that a high rate of hydrogen consumption may be required early in the reaction sequence to a) disrupt dipole-based interactions between the aromatic clusters thus allowing relaxation of the large molecular structures to permit penetration by hydrogen donor solvents and b) cap free radicals formed by homolytic scission of the weaker covalent bonds.

(2) The observation that the conversion of coal to products, grouped as intermediate and low mw, can be precisely represented by an equation derived from kinetics for a series reaction path implies that a) compared to subsequent steps, the rate of formation of high mw products (~1000 amu) is fast, and may result from the scission of weak bonds, and b) the rate limiting steps are the production of intermediate (~500 amu) and low mw (~240 amu) material, formed by the scission of strong bonds.

(3) The observation that the yield of low mw products appears to be somewhat larger than can be explained by the rate-limiting steps of the reaction sequence may be rationalized by the rapid extraction of low mw material entrapped within the coal macromolecular network.

(4) The observation that a single selectivity constant may be used to fit data generated over a range of temperatures indicates that the global activation energies representing the myriad reactions of the two steps representing k_1 and k_2 must be approximately equal. This in turn indicates that similar types of covalent bond breaking mechanisms are involved in the production of low mw products and intermediate mw products. The

selectivity of 1.3 (equal to the ratio of the rate constants k_1/k_2 in equation 7) for the conversion of coal to intermediate and low mw products indicates that high mw material contains bonds that are broken at a faster rate than bonds in the intermediate mw products. This is consistent with the observation that rates of scission of strong bonds joining aromatic structures increase with the size of the aromatic substituents (10,11).
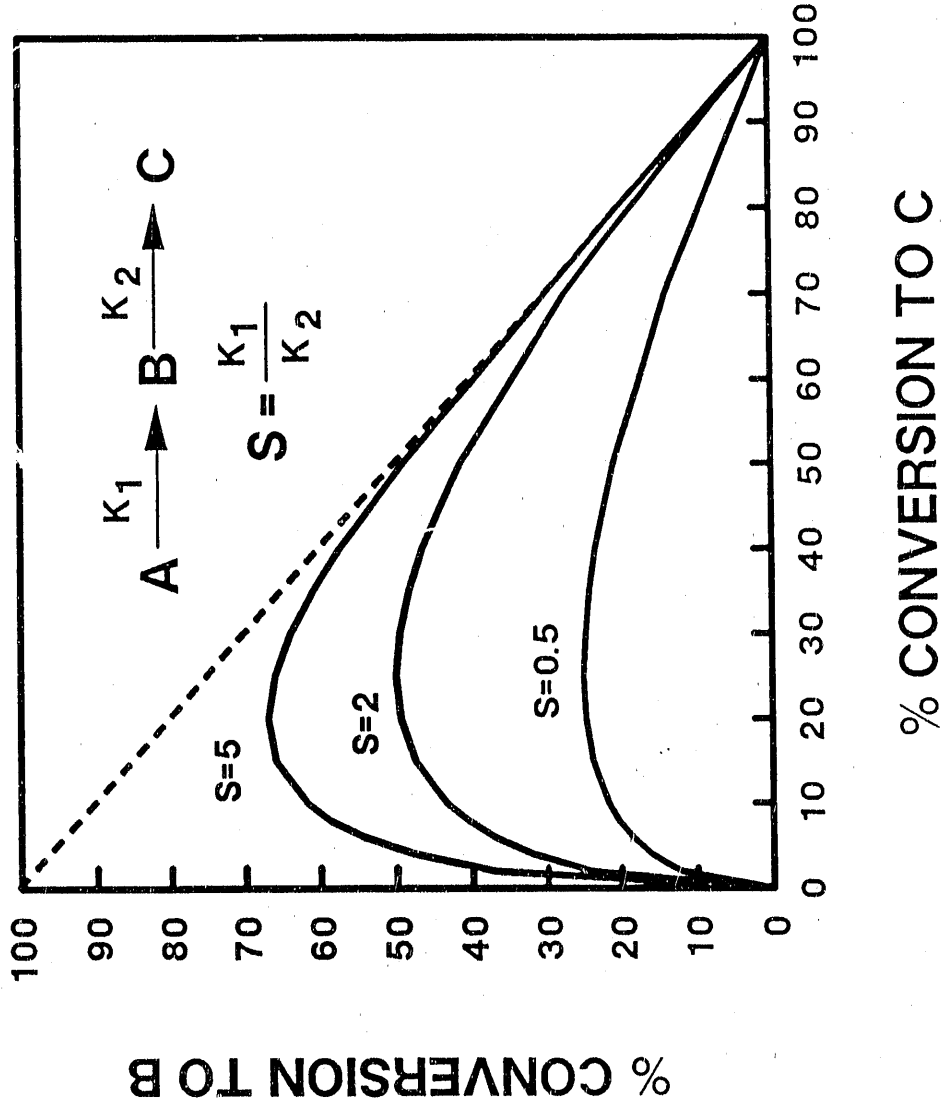
REFERENCES

1. Given, P. H., Marzec, A., Barton, W. A., Lynch, L. J. and Gerstein, B. C., Fuel 65, 155 (1986).

2. Given, P. H. and Marzec, A., Fuel 67, 242 (1988).

3. Lim, R., Davis, A., Bensley, D. F., Derbyshire, F. J., Org. Geochem. 11, 393 (1987).

4. Given, P. H. , Fuel 39, 147 (1960).

5. Wiser, W. H., in Proceedings of the EPRI Conference on Coal Catalysis, Palo Alto, CA, 3 (1973).

6. Solomon, P. R., in New Approaches in Coal Chemistry, ACS Symposium Series No. 169, 61 (1981).

7. Shinn, J. H., Fuel 63, 1187 (1984).

8. Schindler, H. D., Chen, J. M., and Potts, J. D., Integrated Two-Stage Liquefaction, Final Technical Report, DOE Contract DE-AC22-79ET14804, June 1983.

9. Petrakis, I. and Grandy, D. W., Free Radicals in Coals and Synthetic Fuels, Coal Science and Technology 5, Elsevier, Amsterdam (1983).

10. Poutsma, M. L., A Review of Thermolysis Studies of Model Compounds Relevant to Processing of Coal, Oak Ridge National Laboratory Report ORNL/TM--10637, November 1987.

11. Poutsma, M. L., Energy & Fuels 4, 113 (1990).

12. McMillen, D. F., Malhotra, R., Chang, S. J., Fleming, R.H., Ogier, W. C., and Nigenda, S. E., Fuel, 66, 1611 (1987).

13. Malhotra, M. and McMillen, D. F , Energy & Fuels 4, 184 (1990).

14. Stohl, F. V. and Stephens, H. P., I&EC Research 26, 2466 (1987).

15. Chapman, R. N., Coal Liquefaction Preheater Coking--Final Report, Sandia National Laboratories Report SAND83-0248, March, 1983.

16. Kottenstette, R. J., Sandia National Laboratories Report SAND 82-2495, March 1983.

17. Cronauer, D. C., Jewell, D. M., Modi, R. J., Seshadri, K. S., and Shah, Y. T., Isomerization and Adduction of Hydroaromatic Systems at Conditions of Coal Liquefaction, ACS Symposium Series 139, 371, American Chemical Society, Washington, DC (1980).

18. Larsen, J. W., Green, T. K., and Kovac, J., J. Org. Chem., 50, 4729 (1985).

19. Whitehurst, D. D., Mitchell, T. O., and Farcasiu, M. Coal Liquefaction, p. 195, Academic Press (1980).

20. Carlson, G. A., and Granoff, B., ACS Div. of Fuel Chem., Prep. of Papers, 34, No. 3, 780 (1989).

21. Carlson, G. A., personal communication.

22. Larsen, J. A., ACS Div. of Fuel Chem., Prep. of Papers, 33, No. 1, 780 (1988).

23. Breimer, F., Waterman, H. I., and Weber, A. B. R., J. Inst Petroleum, 43, 297 (1957).

24. Waterman, H. I., Bodhouwer, C., and Huibers, D. T. A., Process Characterization, Elsevier, New York (1960).

25. Doelp, L. C., Brenner, W., and Weiss, A. H., I&EC Proc. Des. Dev. 4, 92 (1965).

26. Stephens, H. P., ACS Div. of Fuel Chem., Prep. of Papers, 26, No. 3, 161 (1981).

27. Stephens, H. P., Proceedings of the 1983 International Conference on Coal Science, Pittsburgh, PA, 105 (1983).

28. Derbyshire, F., et al, Fuel 68, 1091 (1989).

29. Neill, P. H., Xia, Y. J., and Winans, R. E., ACS Div. of Fuel Chem., Prep of Papers, 34, No. 3, 745 (1989).

30. Derbyshire, F., Davis, A., and Lin, R., ACS Div. of Fuel Chem., Prep. of Papers, 34, No. 3, 676 (1989).

FIGURE CAPTIONS

Figure 1.   Example of a ternary diagram for a first-order series reaction of the form $A \longrightarrow B \longrightarrow C$. Conversion relationships are shown for several values of the selectivity $S = k_1/k_2$.

Figure 2.   Ternary diagram showing plot of liquefaction conversion data (Table 2) for experiments with an adequate supply of hydrogen. The curve represents an attempt at a least-squares fit of the data to a series reaction path.

Figure 3.   Ternary diagram showing plot of liquefaction conversion data from Table 2 with values for conversion to low mw product reduced by 9%. The curve represents a least-squares fit of the points to a first-order series reaction path.

Fig 1

% CONVERSION TO C

% CONVERSION TO B

Fig 2

% CONVERSION (dmmf coal basis)
TO LOW mw PRODUCT

% CONVERSION (dmmf coal basis)
TO INTERMEDIATE mw PRODUCT

S=1.2

Fig 3.

% CONVERSION (dmmf coal basis)
TO LOW mw PRODUCT

% CONVERSION (dmmf coal basis)
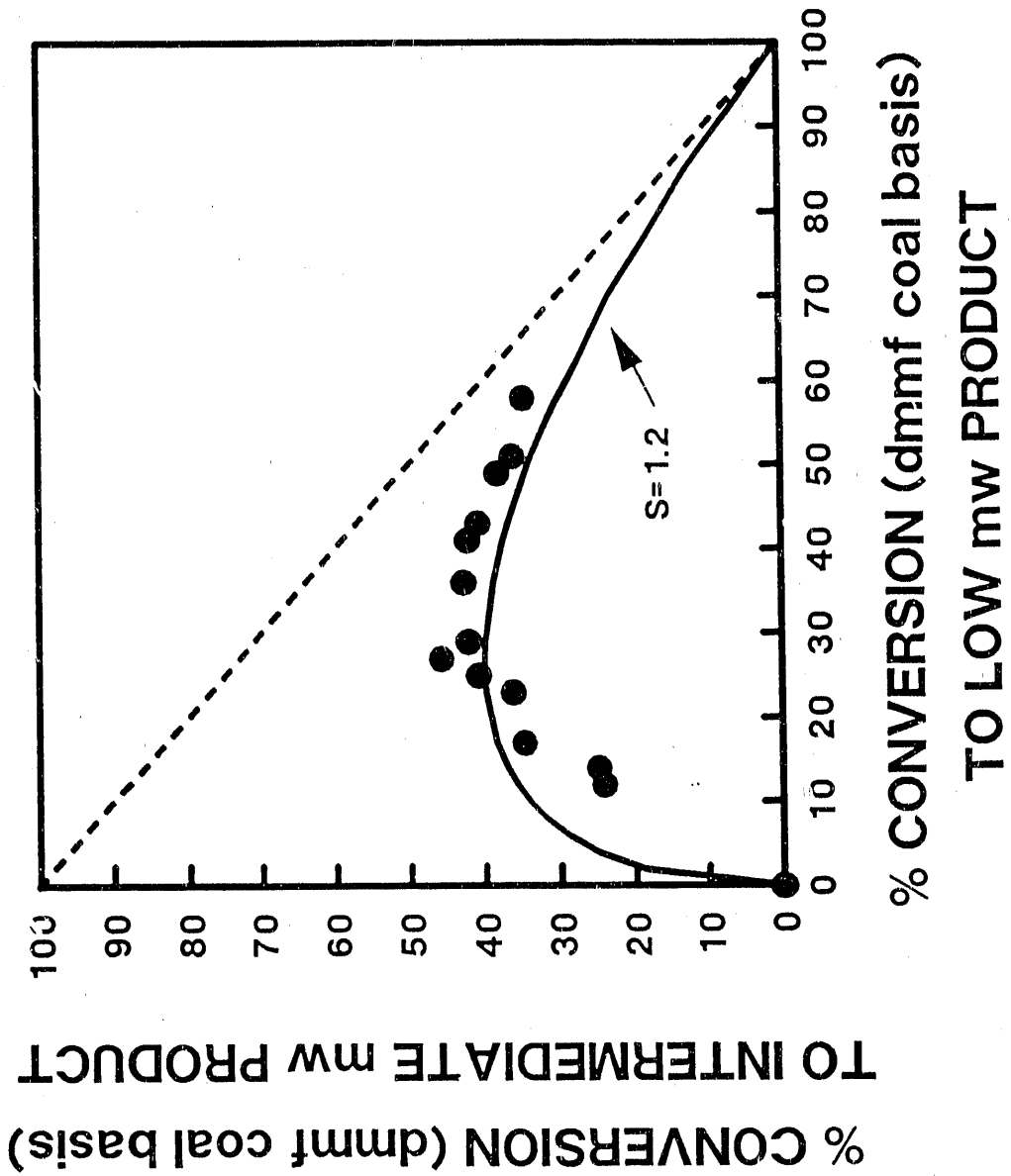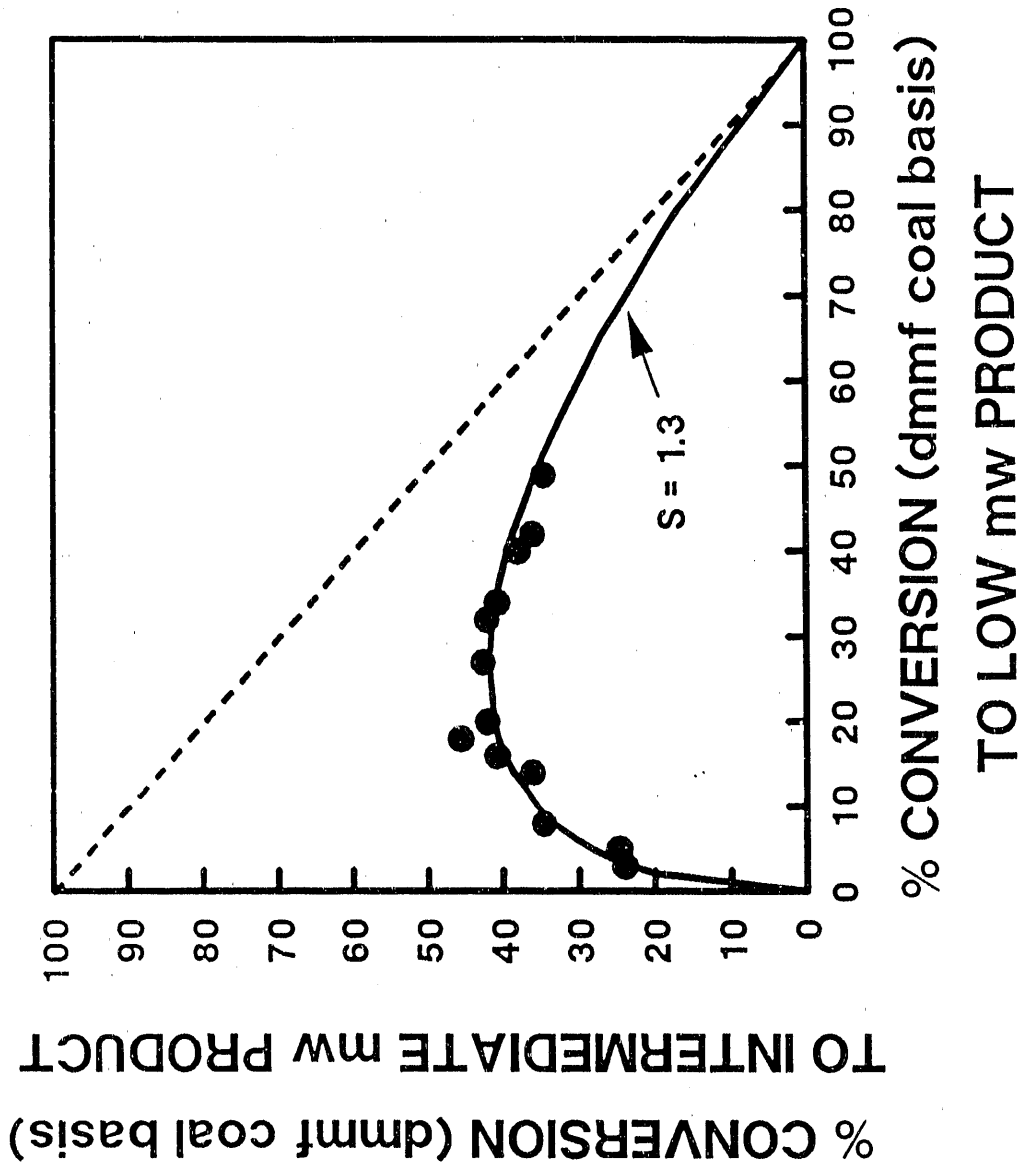TO INTERMEDIATE mw PRODUCT

S = 1.3

Table 1

Reaction Conditions, Product Hydrogen Contents[1] and
Hydrogen Consumption[1] for First Set of Experiments

	Hydrogen Content of Products H/C Ratios and Conversions					Hydrogen Uptake Solvent	H for O, S Removal	Total	Less H in Coal	Calculated Hydrogen Uptake	Experimental Gas Phase H Consumed
	IOM	High	Inter	Low	Gas						
390°C, 10 min, Catalyzed											
H Accounting	8.3	+ 22.8	+ 25.1	+ 14.6	+ 0.4	+ 5.9	+ 0.5	= 77.6	- 62.0	= 15.6	11.8 ± 2
H/C[2]	0.80	0.95	0.97	1.12					0.83		
Conversion[3]	14.5	32.6	34.7	17.2	0.2						
390°C, 10 min, Uncatalyzed											
H Accounting	14.0	+ 26.6	+ 26.3	- 4.2[4]	+ 0.5	+ 2.3	+ 0.2	= 65.7	- 62.0	= 3.7	3,5 ± 2
H/C[2]	0.73	0.94	0.95	1.06					0.83		
Conversion[3]	25.7	40.5	37.3	- 4.7[4]	0.2						
417°C, 30 min, Catalyzed											
H Accounting	1.3	+ 7.6	+ 29.0	+ 37.0	+ 3.5	+ 5.1	+ 1.6	= 85.1	- 62.0	= 23.1	21.1 ± 2
H/C[2]	0.75	0.90	0.95	1.09					0.83		
Conversion[3]	2.5	11.3	40.8	42.9	1.4						
418°C, 30 min, Uncatalyzed											
H Accounting	9.0	+ 7.9	+ 26.1	+ 22.9	+ 3.9	- 1.1[5]	+ 0.7	= 69.4	- 62.0	= 7.4	6.8 ± 2
H/C[2]	0.66	0.87	0.92	1.06					0.83		
Conversion[3]	18.1	12.5	37.9	27.7	2.1						

1. Hydrogen contents and consumptions in mmoles; 2. Atomic ratio; 3. Wt % dmmf coal basis; 4. Due to solvent adduction;
5. Due to hydrogen depletion.

TABLE 2

Reaction Conditions, Product Distribution, and Hydrogen Consumption
for Second Set of Experiments[1]

| | REACTION CONDITIONS | | | | PRODUCT DISTRIBUTIONS | | | | |
| | | | | | (Weight % dmmf) | | | | H₂ Gas[4] |
Exp. No.	Temp (°C)	Time (min)	Solvent[2]	Catalyst	IOM	High	Inter	Low	Consumed
1	368	10	D,2	None	47.4	36.5	25.5	-12.2[3]	0.1
2	390	10	D,2	None	25.7	40.5	37.3	-4.7[3]	0.3
3	393	30	D,2	None	21.5	34.7	44.8	-2.6[3]	0.6
4	426	5	D,2	None	24.0	27.3	36.2	10.2	0.2
5	420	30	D,2	None	18.1	12.5	37.9	27.7	0.6
6	371	10	D,2	Co/Mo	32.7	27.7	24.8	14.0	0.8
7	379	5	D,2	Co/Mo	36.1	26.8	24.1	12.0	0.5
8	390	10	D,2	Co/Mo	14.5	32.6	34.7	17.2	1.0
9	393	30	D,2	Co/Mo	7.7	25.0	40.8	25.0	1.6
10	417	30	D,2	Co/Mo	2.5	11.3	40.8	42.9	1.9
11	416	74	D,2	Co/Mo	2.5	6.2	36.2	51.2	2.1
12	417	30	D,4	None	9.5	16.5	42.1	28.7	0.1
13	415	30	D,4	Co/Mo	∅	10.7	38.2	48.7	0.1
14	415	30	D,8	None	1.4	22.6	45.7	27.1	0.1
15	415	30	D,8	Co/Mo	∅	11.2	34.7	57.5	0.1
16	420	30	C,2	None	5.0	12.5	42.7	36.1	0.2
17	418	30	C,2	Co/Mo	5.3	8.0	42.2	41.2	0.2
18	422	5	C,2	None	11.3	27.8	36.2	22.9	0.0

1. All experiments performed with 5.52 MPa cold charge hydrogen, and 8.00 g total slurry charge.
2. D denotes heavy distillate solvent; C, hydrogenated cresote oil; 2, 4 & 8 denote 2:1, 4:1 and 8:1 solvent to coal ratios.
3. Solvent adduction (solvent consumption or net negative yield of low mw product).
4. Weight percent dmmf coal basis ± 0.1%.

END

DATE FILMED
12 / 26 / 90